Mechanical properties of solid $C_{60}$ studied with density functional tight binding method augmented by an empirical dispersion term



2008 J. Phys.: Condens. Matter 20 275240

(http://iopscience.iop.org/0953-8984/20/27/275240)

IOP PUBLISHING JOURNAL OF PHYSICS: CONDENSED MATTER

J. Phys.: Condens. Matter **20** (2008) 275240 (7pp) doi:10.1088/0953-8984/20/27/275240

# Mechanical properties of solid $C_{60}$ studied with density functional tight binding method augmented by an empirical dispersion term

**Chao Feng[1,2], Chong Zhang[1], Ruiqin Zhang[1], Thomas Frauenheim[3] and Michel A Van Hove[1]**

[1] Department of Physics and Materials Science, City University of Hong Kong, Hong Kong SAR, People's Republic of China
[2] Technical Institute of Physics and Chemistry, Chinese Academy of Sciences, Beijing, People's Republic of China
[3] Bremen Center for Computational Material Science, University Bremen, Bremen, Germany

E-mail: aprqz@cityu.edu.hk (R Zhang)

Received 13 February 2008, in final form 20 May 2008
Published 13 June 2008
Online at stacks.iop.org/JPhysCM/20/275240

**Abstract**

The bulk modulus of solid fcc $C_{60}$ was calculated with a density functional tight binding method, augmented by an empirical van der Waals force. The predicted modulus of 9.1 GPa is in good agreement with the experimental measurements. We found that the geometric structures of $C_{60}$ molecules in the solid fcc phase are considerably changed under strong compression, due to variations in the type of hybridization of carbon atoms. We also observed a reduction of the HOMO–LUMO gap under compression which is attributed to the overlap of $\pi$ orbitals from neighboring $C_{60}$ molecules. Finally, we showed that the dispersion energy correction in the adopted scheme plays an essential role for the quantitative description of the weakly bound $C_{60}$ solid.

(Some figures in this article are in colour only in the electronic version)

## 1. Introduction

Since the identification of the $C_{60}$ molecule [1] and the subsequent discovery of effective synthesis of the $C_{60}$ solid [2, 3], $C_{60}$ has attracted much research interest due to its potential application in electronic and optical nanodevices, as well as in nanoelectromechanical systems. Because of their nanoscale size, the mechanical strength of a nanodevice component, which may be naturally under external stress due to connection and interaction with other components of a device, is a critical parameter that determines the stability of nanodevices. Also, the electronic and thus optical properties of the nanoscale component under applied pressure may be modified, and thus alter the device performance or cause deterioration. Therefore, the exploration of the mechanical stability of solid $C_{60}$ under external stress is needed before it can be successfully used in nanodevice design and fabrication. In particular, as a measure of the material's stiffness, the compressibility or bulk modulus of solid $C_{60}$ has been extensively investigated, using x-ray and neutron diffraction methods and a variety of pressure-transmitting media [4–12]. Based on the available experimental data, however, the results from different groups often differ by significant amounts. The controversy may be attributable to non-hydrostaticity of the pressure generated, the different methods of pressurization and measurements, as well as amorphization, polymerization or phase transition of the sample [12].

Due to the obvious difficulties in the experimental measurements of mechanical properties, theoretical exploration should be performed to establish a reference platform on which future studies, both experimental and theoretical, could be performed. The compression properties of solid $C_{60}$ have been investigated theoretically, mainly using simple empirical intermolecular potentials with Lennard-Jones or exponential atom–

 

atom interactions [4, 13–20]. These calculations were performed primarily to test models for the potentials, and also gave a large variation of the predicted bulk modulus. Furthermore, these molecular mechanics methods cannot be considered as successful in the sense that the empirical intermolecular functions may not be applicable or transferable for $C_{60}$'s derivatives and other complexes. Therefore, theoretical investigations with a higher level of theory are required, which can address the challenges of parametrization and achieve general transferability with a high accuracy.

The intermolecular interactions among $C_{60}$ molecules in the solid phase arise primarily from the weak van der Waals (vdW) type forces, and the long-range dispersion interactions should be the major source of attraction between neighboring $C_{60}$ molecules. Therefore, to obtain quantitative information about weakly bound solid $C_{60}$, the effect of weak intermolecular interactions should be taken into account in the adopted theoretical methods. The most widely used method for this purpose is the second-order Møller–Plesset (MP2) perturbation theory; its application is, however, limited to small systems due to its huge computational demands. Although density functional theory (DFT) often gives accurate solutions for larger clusters or periodic structures, the generally used DFT methods fail to describe the dispersion interaction that contributes significantly to the binding energy. To overcome this drawback, a common practice is to introduce an empirical correction to calculate the additional attraction energy [21–23]. The recently developed self-consistent-charge density functional tight binding (SCC-DFTB) method, augmented by the empirical London dispersion correction (acronym SCC-DFTB-D), follows this approach [24]. In this study, we employed the SCC-DFTB-D method to calculate the bulk modulus of solid fcc $C_{60}$, and compared it with previous experimental measurements and existing calculations. We also investigated the change in the geometry of $C_{60}$ molecules caused by external pressure, as well as the variation of the energy gap with the compression.

## 2. Computational method and models

The SCC-DFTB approach is an approximate DFT scheme, which is derived from a second-order expansion of the Kohn–Sham total energy in DFT with respect to charge density fluctuations. The Hamiltonian matrix elements are calculated with a two-center approximation, which are tabulated together with the overlap matrix elements as a function of the interatomic distance. A comprehensive description of this method can be found in the literature [21, 25]. SCC-DFTB has been proven to be computationally efficient and extremely reliable in the simulation of large systems with hundreds of atoms or periodic materials.

In order to describe the weak interaction between two separated fragments, an empirical dispersion term is added to the SCC-DFTB total energy for large distances, and a damping of this term with the onset of overlap of the charge density is included. The vdW interaction energy is defined as

$$E_{\mathrm{vdw}} = -\sum_{\alpha\beta} f(R_{\alpha\beta}) C_6^{\alpha\beta} (R_{\alpha\beta})^{-6} \tag{1}$$

where $f(R)$ is the damping function as defined in [24],

$$f(R) = [1 - \exp(-d*(R/R_0)^N)]^M \tag{2}$$

with the values $d = 3.0$, $N = 7$ and $M = 4$ for all types of atoms. $R_0$ is defined by the range of the overlap of two atoms, and is taken as 4.8 Å for the second row elements. The $C_6$ coefficient for a given atom $\alpha$ is calculated as

$$C_6^{\alpha} = 0.75\sqrt{N_\alpha p_\alpha^3} \tag{3}$$

where $N_\alpha$ is the Slater–Kirkwood effective number of electrons and $p_\alpha$ is the polarizability of atom $\alpha$. Also

$$C_6^{\alpha\beta} = \frac{2C_6^{\alpha} C_6^{\beta} p_\alpha p_\beta}{p_\alpha^2 C_6^{\alpha} + p_\beta^2 C_6^{\beta}}. \tag{4}$$

In this study, we use the same damping function $f(R)$ and $C_6$ coefficient as used in [24]. The resulting scheme was found to be appropriate for predicting the geometrical structure and binding energy of weakly interacting systems [24, 26, 27].

At room temperature and atmospheric pressure, crystalline $C_{60}$ forms a face-centered-cubic (fcc) phase, in which the $C_{60}$ molecules rotate almost freely and thus are orientationally disordered [28–31]. Many x-ray and neutron diffraction studies of this phase showed that the molecular rotation is not completely free, but that there is an intermolecular orientational correlation [32–36]. For the purpose of computing its compressibility, however, the $C_{60}$ molecule can be thought of as freely rotating with a negligible orientational correlation. Consequently, in the model of solid fcc $C_{60}$ in this study, all $C_{60}$ molecules are oriented with six of their 6–6 double bonds parallel to the supercell vectors, so that their mirror planes are all aligned with the cell faces, as shown in figures 1(a)–(c). In this case, each $C_{60}$ molecule is oriented such that the centers of eight of its twenty hexagons are aligned along the cubic ⟨111⟩ directions, corresponding to the 'standard orientation', which is described in detail in [37]. Therefore, all $C_{60}$ molecules have a unique orientation with respect to their neighboring molecules, i.e. one pentagon of a molecule faces another pentagon of its neighbor with a parallel displacement, as depicted in figure 1(d).

## 3. Results and discussion

The bulk modulus $B$ of a given material can be calculated from

$$B = V_o \frac{\partial^2 E}{\partial V^2}, \tag{5}$$

where $E$ is the total energy, $V$ is the unit cell volume, and $\partial^2 E/\partial V^2$ is the second derivative of $E$ with respect to $V$. Therefore, the variation of the total energy with the unit cell volume, $E(V)$, is required. To this end, we first performed the geometry optimization of an internal $C_{60}$ molecule, which comprises the unit cell of solid fcc $C_{60}$, for a given lattice constant $d$, and thus obtained an optimized geometry of the $C_{60}$ molecule related to the given $d$ and a resulting total energy $E(d)$. Next, we repeated the following procedure: varying $d$

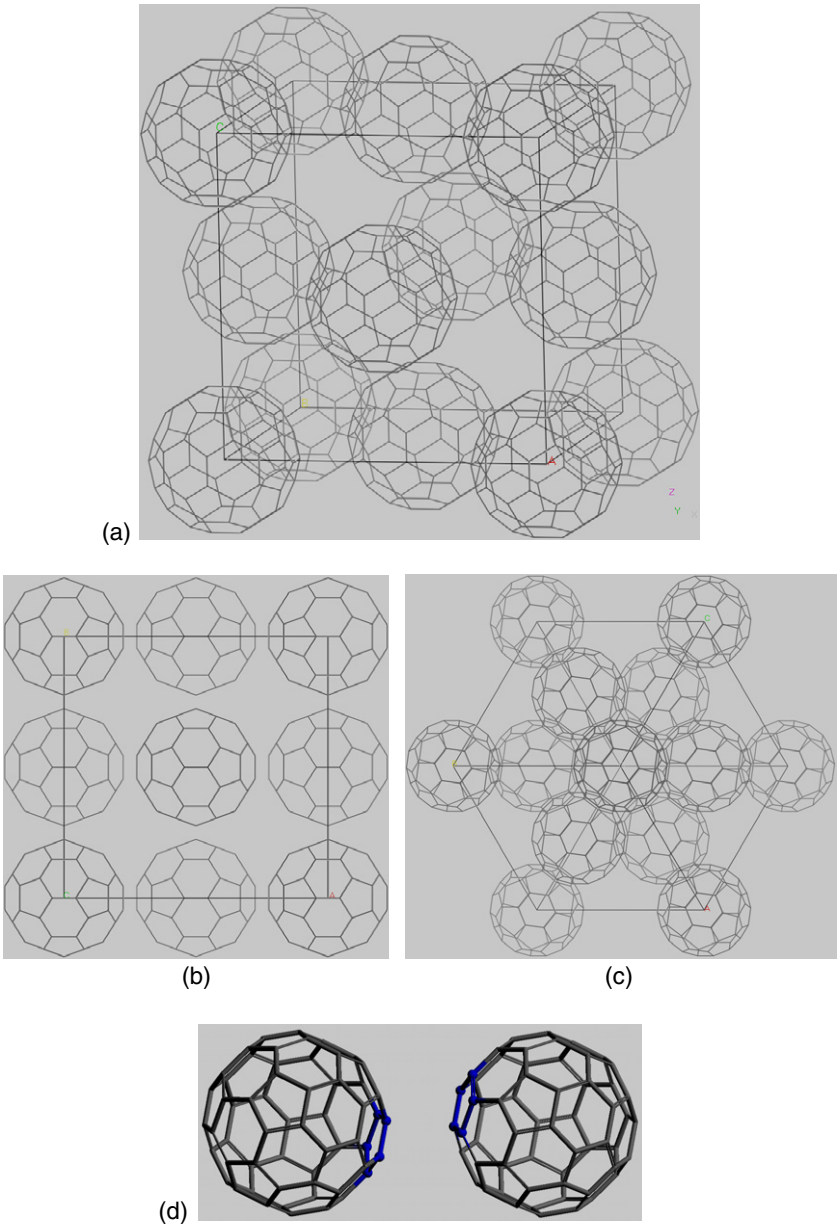


**Figure 1.** (a) The fcc structure of $C_{60}$ in a supercell, and the view along the (b) [001] and (c) [111] direction, respectively. (d) The relative orientation of two neighboring $C_{60}$ molecules with two face-to-face contact pentagons colored in blue.

by small elongations $\delta d$, starting the optimization calculations, obtaining the corresponding total energies as local minima, and determining the global minimum $E_0 = \min_d E(d)$. As a result, we obtained the profile of the function $E(d)$ around the global minimum and the minimal total energy $E_0 = E(d_0)$ at the optimal lattice constant $d_0$ for the most stable structure, as shown in figure 2. Our calculations predict that the optimal lattice constant $d_0$ is 9.9 Å, in good agreement with the measured closest center-to-center $C_{60}$–$C_{60}$ contact distance of 10.0 Å [37], given that the difference of 0.1 Å is of the same order as that at *ab initio* level. Now the total energy curve as a function of the unit cell volume, $E(V)$, can be plotted (see the inset in figure 2), according to the function $E(d)$ and the relation between the fcc unit cell volume and its lattice constant, $V = (\sqrt{2}/2)d^3$. Eventually, the bulk modulus $B$ was calculated to be 9.1 GPa according to equation (4), only about 4.9% lower than the experimental value of 9.6 GPa [36], which was considered as the best estimate of the bulk modulus of solid fcc $C_{60}$ in the low-pressure range, and as the reference standard for theoretical calculations [4]. Our value is much superior compared to the previous theoretical results which used the rather high value of 18.1 GPa [5] as a reference standard [4]. In addition, the SCC-DFTB-D predicted bulk modulus of solid fcc $C_{60}$ indicates that the intermolecular interaction between $C_{60}$ molecules is comparable to the interlayer interaction in graphite, since the $c$-axis compressibility of graphite is $-2.8 \times 10^{-2}$ GPa$^{-1}$ [38], and thus its bulk modulus is close to 33.8 GPa.

In the $C_{60}$ molecule, each carbon atom is $sp^2$ hybridized and bonded to three nearest neighboring carbon atoms with

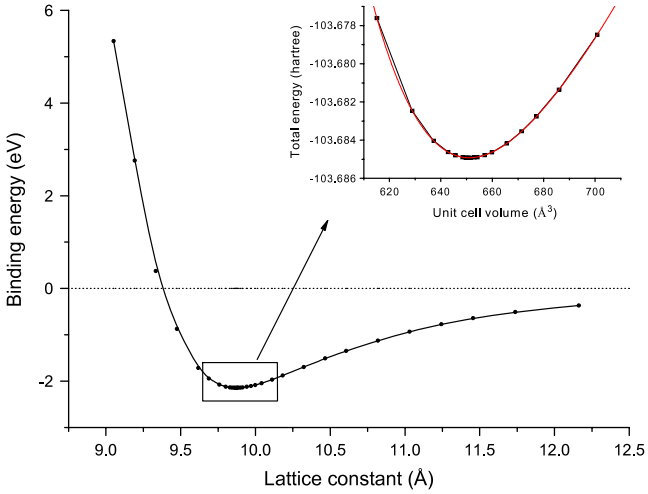


**Figure 2.** Binding energy versus lattice constant. The inset is the total energy curve as a function of the unit cell volume near the global minimum.

$\sigma$ bonds. The remaining valence electron forms a double bond, known as $\pi$ bond, which is delocalized. However, the $C_{60}$ molecule tends to avoid forming double bonds within the pentagonal rings, which makes electron delocalization poor, i.e. the electrons in the hexagonal rings do not completely delocalize throughout the whole cage, resulting in the fact that pentagons are much less aromatic than hexagons. Accordingly, there are two kinds of bonds in the $C_{60}$ molecule, i.e. those between atoms located between pairs of hexagons (short bonds, SB) and those between a hexagon and a pentagon (long bonds, LB). Our calculations predict that the lengths of SBs and LBs at the various locations of $C_{60}$ molecules in the most stable structure of the fcc phase are in the ranges of 1.406–1.408 Å and 1.450–1.456 Å, respectively, both of which are consistent with the corresponding values of 1.407 Å and 1.453 Å in the isolated $C_{60}$ molecule. It can be seen that the lengths of SBs are quite similar to that of the C–C bond within the benzene molecule (1.40 Å), while the lengths of LBs are intermediate between those of the benzene C–C bond and the common C–C single bond. In addition, each carbon atom is bonded to three adjacent carbon atoms, and thus is involved in three bond angles: one is the interior angle of the pentagon ($\alpha$) and the other two are the interior angles of the hexagon ($\beta$). In the most stable structure of solid fcc $C_{60}$, the predicted bond angle $\alpha$ is about 107.9°, and $\beta$ ranges from 119.9° to 120.1°, respectively: those values are close to the corresponding values of 108.0° and 120.0° in an isolated $C_{60}$ cage. Furthermore, the diameter of the $C_{60}$ molecule (i.e. the maximum distance between two C nuclei in one cage) in the optimal fcc structure was calculated to be 6.842 Å, only 0.029 Å smaller than that of an isolated $C_{60}$ molecule. Therefore, we find that the $C_{60}$ molecules shrink slightly when condensed into the solid state under zero pressure.

Under strong compression induced by external pressure, however, the geometries of $C_{60}$ molecules will change considerably, despite the enormous strength of the intramolecular bonds. As shown in figure 3, our calculations reveal that

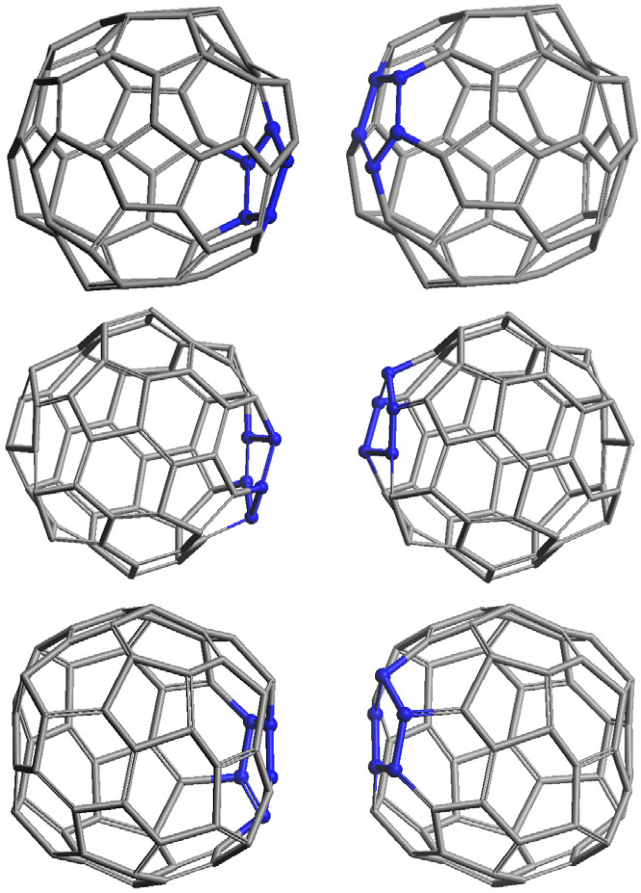

**Figure 3.** 'Wrinkling' of $C_{60}$ molecules in a fcc lattice under strong compression. Pairs of neighboring $C_{60}$ molecules are viewed from three directions, perpendicular to the $\boldsymbol{a}$, $\boldsymbol{b}$ and $\boldsymbol{c}$ unit cell vectors in the top, middle and lower panels, respectively. The two face-to-face contact pentagons are colored in blue to highlight the relative orientation of two neighboring $C_{60}$ molecule.

the geometries of $C_{60}$ molecules are severely 'wrinkled' when the lattice constant is compressed to 8.8 Å, considerably reduced from that at zero pressure. It also can be seen from figure 3 that, although the compression is isotropic, the change in the geometry of the $C_{60}$ cage is anisotropic along three directions of the lattice vectors, due to the anisotropic intermolecular interactions. In this case, the distances between two closest carbon atoms from adjacent $C_{60}$ molecules decrease to 1.39–1.71 Å, indicating the overlap between $\pi$-orbitals from neighboring $C_{60}$ molecules or the possible formation of strong interactions between neighboring $C_{60}$ molecules (see below). The lengths of LBs range from 1.406 to 1.497 Å, while those of SBs range from 1.373 to 1.456 Å, both about 3% different from the values in the most stable structure at zero pressure. It can be seen that the lengths of some bonds are changed to be similar to that of the C–C single bond and the lengths of other bonds tend to be similar to that of the C–C double bond (1.34 Å). On the other hand, the angles $\alpha$ are altered to 100.8°–115.2° and the angles $\beta$ are altered to 103.2°–128.7°, many of which fall in the range from 107° to 111° that is close to the bond angle in the $sp^3$ hybridized orbitals. Therefore, the variations in the bond lengths and bond angles can be elucidated as follows: in

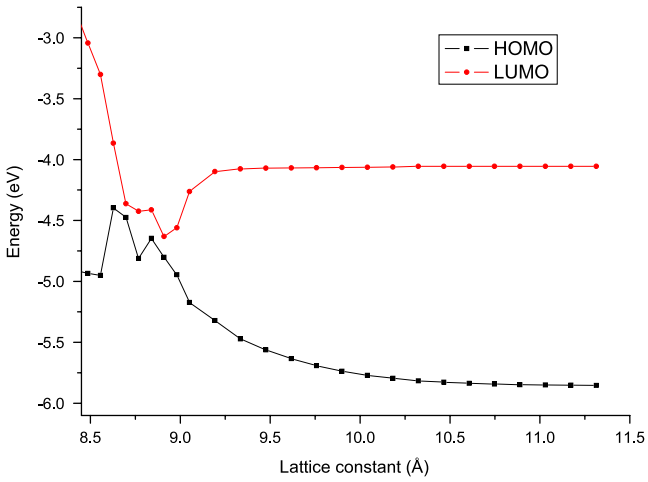


**Figure 4.** Variation of energies of HOMO and LUMO with the lattice constant of fcc $C_{60}$.

the $C_{60}$ molecule the $sp^2$-hybridized carbon atoms, which are at their energy minimum in planar graphite, must be bent to form the closed sphere, thus producing angular strain. Under compression induced by the external stress, however, the angular strain can be reduced by changing partial $sp^2$-hybridized carbons into $sp^3$-hybridized ones, with the redundant orbital overlapped by another from a neighboring $C_{60}$ molecule. The change in hybridized orbitals causes the bond angles to be altered to about 109.5° in $sp^3$ orbitals, which allows the bonds to bend less when closing the sphere. Accordingly, the corresponding bond lengths are changed to be consistent with those of common C–C single and double bonds, and the $\pi$-bonds become more localized, causing the deterioration of aromaticity within the hexagonal rings. Consequently, it can be concluded that the variations in the intramolecular bond lengths and bond angles arise from the changes in the hybridized type of partial carbon atoms and thus in the type of C–C bonding, which results in the distortion of $C_{60}$ molecules.

As was discussed above, the compression under external pressure gives rise to a decrease in intermolecular distance and thus an increase in intermolecular interactions between adjacent $C_{60}$ molecules in the solid phase, which further influences their other properties, for example their electronic properties. It can be seen from figure 4 that the energy of the highest occupied molecular orbital (HOMO) gradually increases when the lattice constant is compressed from about 11.3–8.9 Å, while the energy of the lowest unoccupied molecular orbital (LUMO) slightly decreases. Therefore, the HOMO–LUMO gap decreases drastically from 1.80 to 0.17 eV with the decrease in the intermolecular distance induced by the compression that follows application of pressure. The reduction of the energy gap may arise from the increase in overlap between $\pi$ orbitals from neighboring $C_{60}$ molecules because of the decrease in the contact distance between two cages. It can be observed from figure 5 that, when the lattice constant is compressed to 8.9 Å, the overlap between intermolecular $\pi$ orbitals is much more extensive in comparison with that of the stable structure at zero pressure. On the other hand, when the solid suffers such severe compression, with the closest intermolecular C–C distance of only about 1.49 Å, covalent bonds may be formed between neighboring $C_{60}$ molecules, which will enhance the delocalization of valence electrons and thus reduce the HOMO–LUMO gap. When the lattice constant is compressed

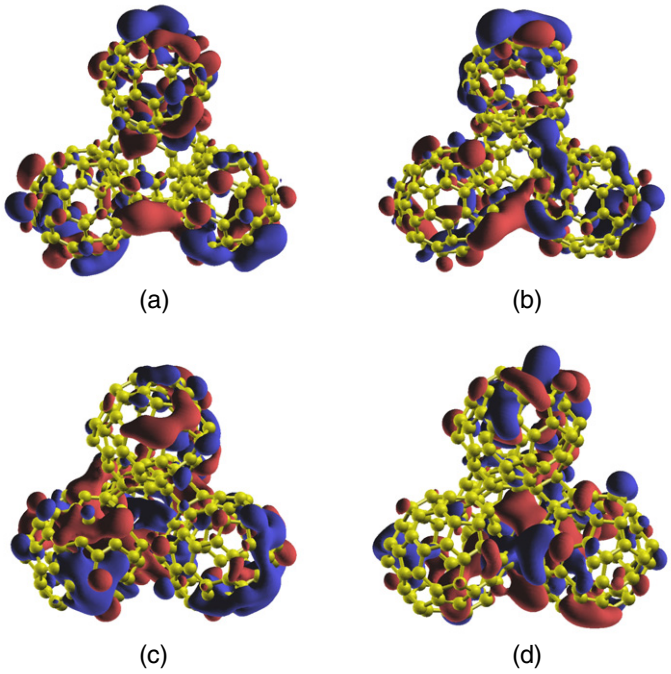


**Figure 5.** Isosurfaces of the wave functions of the HOMOs (left panels) and LUMOs (right panels) derived from bands at the Γ point for the most stable fcc structures of $C_{60}$ in a supercell at zero pressure ($d = 9.9$ Å, upper) and under severe compression ($d = 8.9$ Å, lower), respectively. The iso-value is ±0.02 au. The red and blue colors denote the positive and negative signs, respectively.

below 8.8 Å, however, the energies of HOMO and LUMO change quite dramatically, indicating that solid $C_{60}$ may acquire special distinctive electronic properties under severe external pressure, thus offering the opportunity to tune the material properties by compression.

Finally, to elucidate the crucial effect of weak intermolecular interactions between neighboring $C_{60}$ molecules on stabilizing the $C_{60}$ solid, and the need for the method to be augmented with a dispersion correction in the description of vdW complexes, we compared our results with calculations that omitted the long-range vdW interactions, including the optimization of geometric structures of fcc $C_{60}$ unit cell and the calculation of its structural and mechanical properties using the normal SCC-DFTB scheme without dispersion correction. Being augmented with an empirical term for long distances, the SCC-DFTB-D method predicts that the binding energy of solid fcc $C_{60}$ is as large as $-2.14$ eV per buckyball, as shown in figure 2. In contrast, the SCC-DFTB method does not account for the long-range part of the dispersion interaction, and thus largely underestimates the vdW interaction among $C_{60}$ molecules. It predicts a rather small binding energy of only $-0.05$ eV, indicating that the $C_{60}$ solid state will not quite be stable without dispersion forces, which are thus crucial for the stability of the $C_{60}$ solid. According to equation (5), to calculate the bulk modulus of solid $C_{60}$, the second derivative $\partial^2 E/\partial V^2$ is required, i.e. the theoretical method should provide accurate dependence of total energy $E$ on unit cell volume $V$ or lattice constant $d$. The SCC-DFTB total energy curve is much flatter than that of SCC-DFTB-D (not shown here) in the intermediate distance region in the vicinity of the potential minimum, again due to the missing dispersion correction in the SCC-DFTB total energy. Therefore, the small curvature yields an unreasonably small bulk modulus of only 1.5 GPa, which is much smaller than the previous experimental measurements and the SCC-DFTB-D result, showing that accurate evaluation of the dispersion energy is essential for the quantitative description of the compressibility of vdW complexes. On the other hand, the bulk modulus of a substance is defined as the ratio of the change in pressure to the volume compression. Without dispersion interactions, the $C_{60}$ solid will become unstable as shown above, and be apt to compress under a given amount of external pressure, which will thus result in an unrealistically smaller bulk modulus.

## 4. Conclusions

We calculated the geometric structures and energetics of the fcc $C_{60}$ crystal, using the density functional tight binding method, augmented by an empirical dispersion correction. We predict that the bulk modulus of solid fcc $C_{60}$ is 9.1 GPa, which is consistent with the experimental values and much superior to the results from empirical molecular mechanics calculations. It is revealed that the dispersion forces play a crucial role in the interaction between adjacent $C_{60}$ molecules in the solid state, and that it is essential to take the dispersive energy correction into account in the adopted scheme. When the crystal is compressed by external pressure, i.e. the lattice parameter is considerably contracted, the internal molecular structures are expected to be severely 'wrinkled', accompanied by large changes in the intramolecular bond lengths and bond angles, which are induced by modifications in the hybridization of the carbon atoms. The compression will cause changes in the electronic properties; e.g., the HOMO–LUMO gap decreases from 1.80 to 0.17 eV as the lattice constant is compressed from 11.3 to 8.9 Å, due mainly to the overlap of $\pi$ orbitals on neighboring $C_{60}$ molecules and the formation of covalent bonds between adjacent cages.

## Acknowledgments

The work described in this paper was supported by a grant from the City University of Hong Kong (Project No. 7002030) and by computer time at the CityU Centre for Applied Computing and Interactive Media (ACIM).

## References

[1] Kroto H W, Heath J R, O'Brien S C, Curl R F and Smalley R E 1985 *Nature* **318** 162
[2] Krätschmer W, Lamb L D, Fostiropoulous K and Huffman D R 1990 *Nature* **347** 354
[3] Zhou O and Cox D E 1992 *J. Phys. Chem. Solids* **53** 1373
[4] Sundqvist B 1999 *Adv. Phys.* **48** 1
[5] Duclos S J, Brister K, Haddon R C, Kortan A R and Thiel F A 1991 *Nature* **351** 380
[6] Fischer J E, Heiney P A, McGhie A R, Romanow W J, Denenstein A M, McCauley J P Jr and Smith A B III 1991 *Science* **252** 1288
[7] Lundin A, Sundqvist B, Skoglund P, Fransson A and Pettersson S 1992 *Solid State Commun.* **84** 879
[8] Haines J and Léger J M 1994 *Solid State Commun.* **90** 361
[9] Ludwig H A, Fietz W H, Hornung F W, Gurbe K, Wagner B and Burkhart G J 1994 *Z. Phys.* B **96** 179
[10] Schirber J E, Kwei G H, Jorgensen J D, Hitterman R L and Morosin B 1995 *Phys. Rev.* B **51** 12014
[11] Soifer Ya M, Kobelev N P, Nikolaev R K and Levin V M 1999 *Phys. Status Solidi* b **214** 303
[12] Horikawa T, Kinoshita T, Suito K and Onodera A 2000 *Solid State Commun.* **114** 121
[13] Wang Y, Tomanek D and Bertsch G F 1991 *Phys. Rev.* B **44** 6562
[14] Yildirim T and Harris A B 1992 *Phys. Rev.* B **46** 7878
[15] Li X P, Lu J P and Martin R M 1992 *Phys. Rev.* B **46** 4301
[16] Burgos E, Halac E and Bonadeo H 1993 *Phys. Rev.* B **47** 13903
[17] Yu J, Bi L, Kalia R K and Vashishta P 1994 *Phys. Rev.* B **49** 5008
[18] Zubov V L, Tretiakov N P, Sanchez J F and Caparicia A A 1996 *Phys. Rev.* B **53** 12080
[19] Prilutski Yu I and Shapovalov G G 1997 *Phys. Status Solidi* b **201** 361
[20] Venkatesh R and Gopala Rao R V 1997 *Phys. Rev.* B **55** 15
[21] Elstner M, Porezag D, Jungnickel G, Elsner J, Haugk M, Frauenheim T, Suhai S and Seifert G 1998 *Phys. Rev.* B **58** 7260
[22] Mooij W T M, van Duijneveldt F B, van Duijneveldt-van de Rijdt J G C M and van Eijck B P 1999 *J. Phys. Chem.* A **103** 9872
[23] Wu Q and Yang W T 2002 *J. Chem. Phys.* **116** 515
[24] Elstner M, Hobza P, Frauenheim T, Suhai S and Kaxiras E 2001 *J. Chem. Phys.* **114** 5149
[25] Frauenheim T, Seifert G, Elstner M, Niehaus T, Köhler C, Amkreutz M, Sternberg M, Hajnal Z, Carlo A D and Suhai S 2002 *J. Phys.: Condens. Matter* **14** 3015

[26] Lin C S, Zhang R Q, Lee S T, Elstner M, Frauenheim Th and Wan L J 2005 *J. Phys. Chem.* B **109** 14183
[27] Feng C, Zhang R Q, Dong S L, Niehaus T A and Frauenheim T 2007 *J. Phys. Chem.* C **111** 14131
[28] Heiney P A, Fischer J E, McGhie A R, Romanow W J, Denenstein A M, McCauley J P Jr, Smith A B II and Cox D E 1991 *Phys. Rev. Lett.* **66** 2911
[29] Girifalco L F 1992 *J. Phys. Chem.* **96** 858
[30] Zubov V I, Tretiakov N P, Sanchez J F and Caparica A A 1996 *Phys. Rev.* B **55** 12080
[31] Bohnen K P and Heid R 1999 *Phy. Rev. Lett.* **83** 1167
[32] Pintschovius L 1996 *Rep. Prog. Phys.* **57** 473
[33] Chow P C, Jiang X, Reiter G, Wochner P, Moss S C, Axe J D, Hanson J C, McMullan R K, Meng R L and Chu W W 1992 *Phys. Rev. Lett.* **69** 2943
[34] David W I F, Ibberson R M and Matsuo T 1993 *Proc. R. Soc.* A **442** 129
[35] Pintschovius L, Chaplot S L, Roth G and Heger G 1995 *Phys. Rev. Lett.* **75** 2843
[36] Pintschovius L, Blaschko O, Krexner G and Pyka N 1999 *Phys. Rev.* B **59** 11020
[37] Rosseinsky W J 1995 *J. Mater. Chem.* **5** 1497
[38] Hanfland M, Beister H and Syassen K 1989 *Phys. Rev.* B **39** 12598